doi:10.3788/gzxb20144310.1006001

双光程光纤陀螺的温度致非互易性研究

徐宏杰,张文艳,徐小斌,宋凝芳

(北京航空航天大学 仪器科学与光电工程学院,北京 100191)

摘 要:为了提高陀螺的精度,提出了一种新型双光程光纤陀螺.在光纤环两端各连接一个偏振分束器,使得偏振光依次沿保偏光纤的快轴、慢轴传输两圈,其有效光程加倍,进而实现陀螺的 Sagnac 效应加倍.针对该光纤陀螺在温度场扰动下的非互易问题,分析了其特殊结构带来的温度致非互易误差,利用有限元分析法建立了相应的 Shupe 误差模型,并对光纤环 90°熔点位置、光纤环折射率温度系数改变对 Shupe 误差影响进行了相应的理论计算与仿真分析,结果表明 90°熔点置于光纤环中点或者选用折射率温度系数满足特定条件的光纤环可减小其 Shupe 误差.

关键词:光纤陀螺;Shupe 误差;有限元;保偏光纤环;双光程

中图分类号:V241.533 **文献标识码**:A **文章编号**:1004-4213(2014)10-1006001-5

Research on Thermal Induced Non-reciprocity in Fiber-optic Gyroscope with Double Optical Length

XU Hong-jie, ZHANG Wen-yan, XU Xiao-bin, SONG Ning-fang

(*School of Instrument Science and Opto-electronics Engineering, Beijing University of Aeronautics and Astronautics, Beijing* 100191, *China*)

Abstract: In order to improve the precision of fiber-optic gyroscope, a novel fiber optic-gyroscope with double optical length was presented. By employing two polarization beam splitters, polarized light propagated twice along the slow and fast axes of the polarization maintaining fiber sensing coil in sequence to double its effective optical length and precision further. The thermal induced non-reciprocity in the proposed fiber-optic gyroscope was analyzed according to its special structure. With finite element analysis technique, modeling and simulation of the Shupe bias errors were also conducted. By modifying the 90°splicing point to the middle of the sensing coil or choosing appropriate fiber with special refractive index temperature coefficients , the Shupe bias error can be reduced significantly, which is low enough to meet the requirement of fiber optic-gyroscopes with high performance.

Key words: Fiber optic-gyroscope; Shupe bias error; Finite element; Polarization maintaining fiber coil; Double optical length

OCIS Codes: 060.2800; 060.2420; 060.2370; 060.2310; 060.2380

0 Introduction

Fiber-Optic Gyroscope (FOG) is a kind of angle velocity sensor based on Sagnac effect[1]. With characteristics of high precision, solid structure, high reliability and fast startup, it has been widely used in navigation and guidance fields[2-3]. As the requirement of miniaturization and high precision of FOGs increasing, the contradiction between its weight, size and precision is highlighted. In recent years, application of both birefringent axes in Polarization Maintaining Fiber (PMF) sensing coil which form two

Foundation item: The National Natural Science Foundation of China (No. 61205077)

First author: XU Hong-jie(1968—), male, associate professor, Ph. D. degree, mainly focuses on fiber optic-gyroscope, new fiber optic sensing technology and special fiber optic device design. Email:18911906570@189.cn

Responsible author(Corresponding author): ZHANG Wen-yan(1990—), female, M. S. degree candidate, mainly focuses on fiber optic-gyroscope fiber technology. Email:ywzwy123@126.com.

Received: Jan. 14, 2014; **Accepted**: Mar. 28, 2014

FOGs in a single optical coil has been reported. Slow and fast axes have been simultaneously used in a frequency modulated continuous wave gyroscope[4-5] and a resonant FOG[6]. However, this method is still in an experimental stage because of the complicated signal demodulation algorithm, the strong Rayleigh scattering and the Kerr effect occurring[7-8] in the resonant cavity[9].

In order to increase the sensitivity of FOG, without increasing the length or diameter of the PMF sensing coil, a novel fiber optic-gyroscope with double optical length is proposed. By employing two polarization splitters, polarized light propagates twice along the slow and fast axes of the PMF sensing coil in sequence so that the optical length can be doubled. So this new kind of FOGs have several advantages, such as double sensitivity, small size and improved vibration stability[10], which can be applied to cases in miniaturization and high precision.

1 Basic principle of the new FOG

1.1 Structure of the new FOG

The proposed FOG structure is shown in Fig. 1 which consists of an Amplified Spontaneous Emission (ASE) light source, a fiber coupler, a Y integrated waveguide, two Polarization Beam Splitters (PBS), a polarization maintaining fiber sensing coil, a photo detector, and a digital electronic circuit. The polarization maintaining fiber sensing coils are combined with two pigtailed polarization beam splitters (PBS_1 and PBS_2). For each PBS, the slow and fast axes of their common pigtail fiber are respectively aligned with the fast axis of its two branch pigtail fibers. And there is a 90° fiber splicing point in somewhere of the PMF sensing coil.

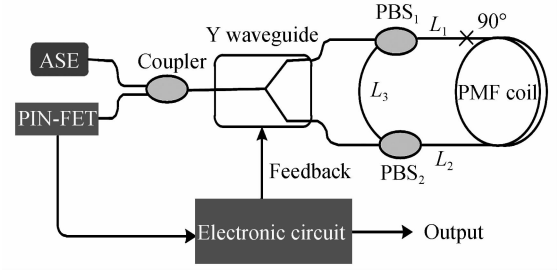

Fig. 1 Typical structure of the new FOG

Assuming the linear polarized light emitted by ASE light source travels through the coupler, Y waveguide along fast axis of the polarization maintaining fiber, then the induced light enters into the PMF sensing coil in clockwise and counter-clockwise and propagates through the fast axis and slow axis of the PMF coil twice in sequence and experiences different optical paths.

1.2 Optical length model

The corresponding effective optical path is shown in Fig 2.

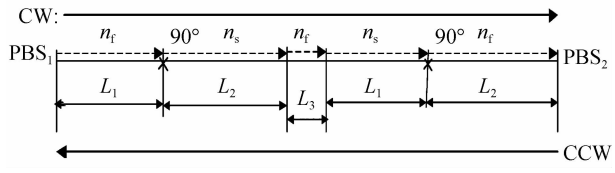

Fig. 2 Effective optical length of clockwise and counter-clockwise light wave

The effective optical length of the Clockwise(CW) and Counter-clockwise(CCW) light in the polarization maintaining fiber sensing coil are both $n_f L_1 + n_s L_2 + n_f L_3 + n_s L_1 + n_f L_2$, where n_f and n_s represent refractive index of fast axis and slow axis respectively, L denotes the geometric length of the PMF coil, L_1 is the length between PBS_1 and 90° splicing point, L_2 is the length between PBS_2 and 90° splicing point, L_3 is the length between PBS_1 and PBS_2. The optical path length difference between CW and CCW light waves in the above PMF sensing coil is equal to zero. And the optical lengths of CW and CCW light waves are reciprocity.

Although the optical length of CW and CCW light waves is reciprocity, the non-reciprocity induced by temperature on optical length in PMF coil should be considered for practical use.

2 Numerical model of thermal induced non-reciprocity in the new FOG

The Shupe effect in the conventional PMF coil has already been analyzed in the previous works. As described by Shupe[11], the conventional FOG is susceptible to a non-reciprocity effect caused by the thermal gradient in non-reciprocity position of the fiber coil[12-13]. As shown in Fig. 3, when the ambient temperature of FOG changes with a speed of $\partial T/\partial t$,

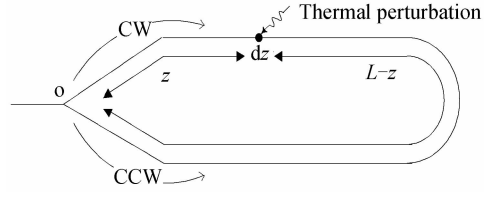

Fig. 3 The PMF sensing coil under temperature

the non-reciprocity phase difference between the CW and CCW waves due to transient effect in conventional FOG can be expressed as follows

$$\Delta\varphi_e(z)=\frac{2\pi}{\lambda}\frac{\mathrm{d}n}{\mathrm{d}T}\int_0^L\frac{\partial T}{\partial t}(z)\frac{L-2z}{c}\mathrm{d}z \tag{1}$$

where $\Delta\varphi_e$ denotes the Shupe bias error, λ is the wavelength of light emitted by the light source, is the effective refractive index, $\mathrm{d}n/\mathrm{d}T$ is the refractive index temperature coefficient, $\partial T/\partial t$ is the time derivative of

the temperature, L is the length of the sensing coil.

Shupe effect in the new FOG should be based on the studies of conventional FOG[14-15]. When the ambient temperature of FOG changes with a speed of $\partial T/\partial t$, suppose that the combined pigtail length of the two PBS are small enough to be merged into the length of the PMF coil, according to Eq. (1), the thermal induced phase error of CW light wave can be given as

$$\begin{aligned}\varphi_{CW} &= \beta_0 n_f L_1 + \beta_0 n_s L_2 + \beta_0 n_f L_3 + \beta_0 n_s L_1 + \beta_0 n_f L_2 + \\ &\beta_0 \frac{\partial n_f}{\partial T}\int_0^{L_1} \Delta T\left(z, t - \frac{L_1 - z}{c/n_f}\right)dz + \beta_0 \frac{\partial n_s}{\partial T}\int_{L_1}^{L_1+L_2} \Delta T\left(z, t + \right. \\ &\left.\frac{z - L_1}{c/n_s}\right)dz + \beta_0 \frac{\partial n_f}{\partial T}\int_{L_1+L_2}^{L_1+L_2+L_3} \Delta T\left(z, t + \frac{L_2}{c/n_s} + \right. \\ &\left.\frac{z - L_1 - L_2}{c/n_f}\right)dz + \beta_0 \frac{\partial n_s}{\partial T}\int_0^{L_1} \Delta T\left(z, t + \frac{L_2 + z}{c/n_s} + \right. \\ &\left.\frac{L_3}{c/n_f}\right)dz + \beta_0 \frac{\partial n_f}{\partial T}\int_{L_1}^{L_1+L_2} \Delta T\left(z, t + \frac{L_1 + L_2}{c/n_s} + \right. \\ &\left.\frac{z - L_1 + L_3}{c/n_f}\right)dz \end{aligned} \tag{2}$$

where β_0 is the propagation constant in vacuum, $\partial n_f/\partial T$ and $\partial n_s/\partial T$ are the fast and slow refractive index temperature coefficients respectively, $\Delta T(z, t_i)$ denotes the change temperature at time t_i and the distance z. The thermal induced phase error for CCW light wave can be given as

$$\begin{aligned}\varphi_{CCW} &= \beta_0 n_f L_1 + \beta_0 n_s L_2 + \beta_0 n_f L_3 + \beta_0 n_s L_1 + \beta_0 n_f L_2 + \\ &\beta_0 \frac{\partial n_f}{\partial T}\int_0^{L_1} \Delta T\left(z, t + \frac{L_2 - L_1}{c/n_f} + \frac{L_1 - z}{c/n_s}\right)dz + \\ &\beta_0 \frac{\partial n_s}{\partial T}\int_{L_1}^{L_1+L_2} \Delta T\left(z, t + \frac{L_2 - z}{c/n_f}\right)dz + \\ &\beta_0 \frac{\partial n_f}{\partial T}\int_{L_1+L_2}^{L_1+L_2+L_3} \Delta T\left(z, t + \frac{L_1}{c/n_s} + \frac{2L_2 + L_3 - z}{c/n_f}\right)dz + \\ &\beta_0 \frac{\partial n_s}{\partial T}\int_0^{L_1} \Delta T\left(z, t + \frac{L_2 + L_1}{c/n_s} + \frac{L_3 + L_2 - z}{c/n_f}\right)dz + \\ &\beta_0 \frac{\partial n_f}{\partial T}\int_{L_1}^{L_1+L_2} \Delta T\left(z, t + \frac{L_2 + L_3 - L_1}{c/n_f} + \right. \\ &\left.\frac{2L_1 + L_2 - z}{c/n_s}\right)dz \end{aligned} \tag{3}$$

The Shupe bias error is the difference thermal induced phase between CW light and CCW light. By simplifying, temperature variation $\Delta T(z, t_i)$ can be converted into temperature gradient $\Delta \dot{T}(z)$, and the thermal induced non-reciprocity phase can be expressed as

$$\begin{aligned}\Delta\varphi_e &= \varphi_{CW} - \varphi_{CCW} \\ &\frac{\beta_0}{c}\frac{\partial n_f}{\partial T}\left\{\int_0^{L_1} \Delta \dot{T}(z)\left[n_f(2z - L_1 - L_2 - L_3) - \right.\right. \\ &\left. n_s(L_1 + L_2)\right]dz + \int_{L_1}^{L_1+L_2} \Delta \dot{T}(z)\left[n_f(2z - L_1 - \right. \\ &\left. L_2 + L_3) + n_s(L_1 + L_2)\right]dz + \int_{L_1+L_2}^{L_1+L_2+L_3} \Delta \dot{T}(z) \cdot \\ &\left[n_f(2z - L_1 - 3L_2 - L_3) + n_s(L_2 - L_1)\right]dz\} + \\ &\frac{\beta_0}{c}\frac{\partial n_s}{\partial T}\left\{\int_0^{L_1} \Delta \dot{T}(z)\left[n_f(L_1 - L_2 + L_3) + \right.\right. \\ &\left. n_s(2z - L_1 + L_2)\right]dz + \int_{L_1}^{L_1+L_2} \Delta \dot{T}(z)\left[n_f(L_1 - \right. \\ &\left.\left. L_2 - L_3) + n_s(2z - 3L_1 + L_2)\right]dz\right\} \end{aligned} \tag{4}$$

Actually, the length between PBS_1 and PBS_2 is small enough so that we can neglect its influence on the total thermal induced phase of the new FOG. From the form of Eq. (4), the Shupe bias error in the new FOG is still the length of the PMF coil for integral, but is divided into three segments L_1, L_2, L_3 respectively integral. And that is approximately equal to the sum of Shupe effect in two conventional FOGs (one transmits in fast axis and the other transmits in slow axis).

Considering an ideal situation, when the temperature changes with the same speed in everywhere of the PMF sensing coil, Shupe bias error of conventional FOGs is zero. However, for the new FOG, Eq. (4) can be transformed as

$$\begin{aligned}\Delta\varphi_e = \frac{\beta_0}{c} \cdot \frac{\partial T}{\partial t}\left[\left(\frac{\partial n_f}{\partial T} \cdot n_s - \frac{\partial n_s}{\partial T} n_f\right)(L_1 - L_2) \cdot \right. \\ \left.(L_1 + L_2 + L_3)\right] \end{aligned} \tag{5}$$

As shown in Eq. (5), the Shupe bias error of the proposed FOG is different from conventional Shupe effect in that the special thermal induced phase error is caused by its unique structure, in general, non-zero. It can be eliminated completely when the 90° splicing point is at the middle of the PMF sensing coil.

3 Simulation and analysis

3.1 Simulation under different position of 90° splicing point

In order to analyze the Shupe bias error of the proposed fiber optic-gyroscope, the thermal induced non-reciprocity model of the proposed FOG is simulated in this part. With finite element analysis method, we simulate the Shupe bias error under the condition of different position of 90° splicing point. The parameters that we used for simulation are listed in Table 1. Assuming that the heat source is outside the PMF sensing coil and the length difference between adjacent layers of the PMF coil are 0.1 m, 90° splicing point is at one end of the layer, the temperature changing rate of L_3 is the same with the most outer sphere of PMF coil. As shown in Table 1, $\Delta \dot{T}(z)$ is the gradient of the temperature changing rate, the temperature changing rates of PMF coil inlayer and outer sphere are 0.061℃/s and 0.1℃ respectively, in addition, different temperature changing rate per layer is 0.001℃/s.

The simulation results under different position of 90° splicing point are shown in Fig. 4. By applying a quadrupolar winding pattern to the PMF coil, the

Shupe bias error is less than 2×10^{-6} rad, much smaller than 1.3×10^{-3} rad simulated by cylinder winding, which is accord with conversational FOG. Simulation results also indicate that the thermal-induced phase would be divergent obviously when the 90°splicing point is in different position.

Table 1 Simulation parameters

Parameters	Value
PMF oil layers	40
L/m	600
L_3/m	0.2
λ/nm	1 550
n_s	1.464 8
n_f	1.464 4
$\partial n_s/\partial T$/℃$^{-1}$	1×10^{-5}
$\partial n_f/\partial T$/℃$^{-1}$	1×10^{-5}
$\Delta\dot{T}(z)$/(℃ s^{-1})	0.061 : 0.001 : 0.1

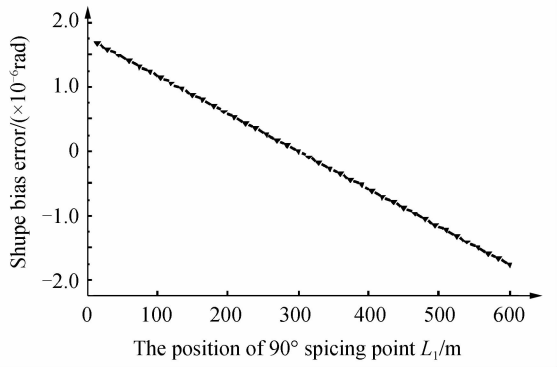

Fig. 4 Simulation results under different position of 90°splicing point

In particular, the thermal induced non-reciprocity with a 90° splicing point at midpoint is almost zero, which is much slower than that with a 90°splicing point at one end. Because when the 90°splicing point is in the middle of fiber coil, the temperature variation is equal at symmetry points, the two counter-propagating waves are in the same axes and experience same refractive index, non-reciprocity induced by temperature (the Shupe bias error) can be reduced completely under the condition of ideal quadrupolar winding pattern.

3.2 Simulation under different refractive index temperature coefficients

Actually, it is difficult to place the 90° splicing point exactly at the middle of fiber coil and the quadrupolar winding in fabrication of the fiber coil is non-ideal, the thermal induced error cannot be completely eliminated just through modifying the position of 90°splicing point to the middle of fiber coil. That means the Shupe bias error can also be considerably reduced by this mean, and it will be suppressed by another effective approach.

From the Eq. (4), it can be concluded that the Shupe bias error is also influenced by refractive index temperature coefficients $\partial n_f/\partial T$ and $\partial n_s/\partial T$. So we simulate the Shupe bias error under different fast and slow refractive index temperature coefficients further. The simulation parameters of refractive index temperature coefficients are listed in Table 2 and other parameters setting value are same to the mentioned above in Table 1. The simulation results are presented in Fig 5.

Table 2 Refractive index temperature coefficients($\times10^{-5}$℃$^{-1}$)

Parameters	a_1	a_2	b	c_1	c_2
$\partial n_f/\partial T$	−1.05	−1.03	0.999 727	1.03	1.05
$\partial n_s/\partial T$	1	1	1	1	1

As shown in Fig. 5 (a), the two curves of a_1 and a_2 are almost coincident, when the sign of $\partial n_f/\partial T$ and $\partial n_s/\partial T$ are opposite, the Shupe bias error is so high that it cannot be applied in practice. When the sign of the fast and slow refractive index temperature coefficient are both positive, the Shupe bias error grows with the increase in their difference value, e. g., the thermal induced non-reciprocity in c_2 is much higher than that in c_1. In particular, when $n_s\cdot\partial n_f/\partial T=n_f\cdot\partial n_s/\partial T$

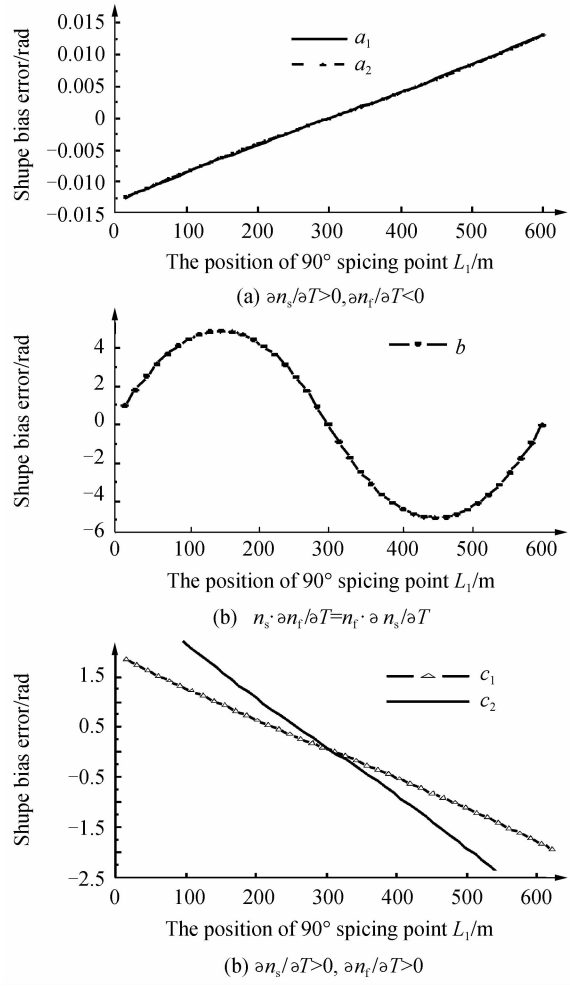

Fig. 5 Influence of different refractive index temperature coefficients on Shupe bias error

$\partial n_s/\partial T$, as shown in Fig. 5(b), the Shupe bias error maximum is 5×10^{-8} rad which is four orders of magnitude less than that in c_1 and c_2. Because when $\partial n_f/\partial T$ and $\partial n_s/\partial T$ are both positive, the thermal induced non-reciprocity phase in the first lap and the second lap are opposite. Therefore, the Shupe bias error would be suppressed by adopting appropriate PMF sensing coil according with $n_s \cdot \partial n_f/\partial T = n_f \cdot \partial n_s/\partial T$.

4 Conclusion

In this paper, we propose a new type of fiber optic-gyroscope with double optical length by combining two PBS with the polarization maintaining fiber sensing coil. It has advantages of double sensitivity, small size and high precision. Simulation results and theoretical analysis illustrate unequivocally that by modifying the 90°splicing point to the middle of fiber coil has the significant advantage to reduce its thermal sensitivity. And the Shupe bias error in the new fiber-optic gyroscope can also be greatly suppressed by choosing appropriate PMF sensing coil whose refractive index temperature coefficients accord with $n_s \cdot \partial n_f/\partial T = n_f \cdot \partial n_s/\partial T$. The work supplies theoretical foundation for the reduction of Shupe bias error in the new fiber-optic gyroscope. However, the bias error in the new FOG is affected by many factors, i. e., stress, polarization error. The bias error generated by the two PBS and polarization error caused by crossovers in the fiber-optic gyroscope with double optical length will be discussed in a future research.

References

[1] LEFEVRE H C. The fiber-optic gyroscope[M]. London: Artech House, 1993, 28-58.

[2] LEFEVRE H C. The fiber-optic gyroscope: challenges to become the ultimate rotation-sensing technology[J]. *Optical Fiber Technology*, 2013, **19**(6): 828-832.

[3] NAYAK J. Fiber-optic gyroscope: from design to production [J]. *Applied Optics*, 2011, **50**(25): 152-161.

[4] ZHENG J. Birefringent fiber frequency-modulated continuous-wave Sagnac gyroscope[J]. *Electronics Letters*, 2004, **40**(24): 1520-1522.

[5] ZHENG J. Differential single mode fiber frequency modulated continuous-wave Sagnac gyroscope[J]. *Electronics Letters*, 2005, **41**(13): 727-728.

[6] PINNOJI P D, NAYAK J. Design and analysis of a dual-axis resonator fiber-optic gyroscope employing a single source[J]. *Applied Optics*, 2013, **52**(22): 5350-5354.

[7] TAKIGUCHI K, HOTATE K. Method to reduce the optical Kerr-effect induced bias in an optical passive ring- resonator gyro[J]. *Optical Fiber Sensors*, 1992, **4**(2): 203-206.

[8] YAO Qiong, HU Yong-ming, SONG Zhang-qi, *et al*. Research on the elimination of Kerr effect in resonator fiber optic-gyroscope[J]. *Acta Photonica Sinica*, 2005, **34**(9): 1320-1323.

[9] YAO Qiong, SONG Zhang-qi, XIE Yuan-ping, *et al*. Study on the resonance characteristics of fiber optic ring in resonator fiber optic gyroscope[J]. *Acta Photonica Sinica*, 2007, **36**(4): 676-680.

[10] LI Chang-sheng, ZHANG Chun-xi, SONG Ning-fang, *et al*. Polarization-maintaining fiber loop with double optical length and its application to fiber optic gyroscope[J]. *Chinese Optics Letters*, 2011, **9**(2): 1498-1550.

[11] SHUPE D M. Thermally induced non-reciprocity in the fiber-optic interferometer[J]. *Applied Optics*, 1980, **19**(5): 654-655.

[12] LOFTS C M, PARKER M D, SUNG C C. Investigation of the effects of temporal thermal gradients in fiber optic gyroscope sensing coils[J]. *Optical Engineering*, 1995, **34**(10): 2856-2863.

[13] MOHR F. Thermo-optically induced bias drift in fiber optical Sagnac interferometers[J]. *Lightwave Technology*, 1996, **14**(1): 27-41.

[14] CHEN Xi-yuan, SHEN Chong. Study on error calibration of fiber optic-gyroscope under intense ambient temperature variation [J]. *Applied Optics*, 2012, **51**(17): 3755-3762.

[15] LI Yan, XU Hong-jie, ZHANG Chun-xi. Study on the thermal-induced non-reciprocity of sensing coil of FOG[J]. *Optical Technique*, 2006, **32**(5): 770-772.